JOURNAL OF CATALYSIS 131, 502–512 (1991)

Oxidative Leaching of Cu Atoms from PdCu Particles in Zeolite Y

ZONGCHAO ZHANG, LIQIANG XU, AND WOLFGANG M. H. SACHTLER

V. N. Ipatieff Laboratory, Northwestern University, Evanston, Illinois 60208, U.S.A.

Received January 15, 1991; revised March 12, 1991

NaY-supported PdCu samples of various Cu/Pd ratios were prepared by ion exchange with $Pd(NH_3)_4^{2+}$ and $Cu(NH_3)_4^{2+}$ precursors. Reduction of Cu is enhanced by Pd; however, after calcination at 500°C the bare ions have migrated into sodalite cages, and reduction is only enhanced for those Cu^{2+} ions which happen to share their cage with a Pd^{2+} ion. Reduction with H_2 results in bimetallic PdCu particles and protons of high Brønsted acidity. At 280°C, and in an inert atmosphere, these protons selectively reoxidize surface Cu atoms to Cu^+ ions, which are still attached to the surface of the bimetal particles; they can be reduced at 210°C. Complete oxidation of the Cu component takes place at 500°C; the Cu^{2+} ions leached from PdCu particles migrate to small zeolite cages, as indicated by EXAFS and a peak at 290°C in the profile of subsequent TPR. After complete leaching of Cu, the monometallic Pd particles are discerned from the original particles in PdCu/NaY and $PdCu_2$/NaY by their propensity to form hydrides that are detectable by TPD. No hydride is formed with bimetal particles with Cu/Pd > 0.5; particles in Pd_2Cu/NaY do form a hydride which is, however, distinguished from Pd hydride by its TPD peak position.

I. INTRODUCTION

Bimetal catalysts, comprising a combination of atoms of a group VIII metal and a group IB metal, have been instrumental in identifying the "ensemble effect" in catalytic reactions such as hydrogenolysis (*1–4*). The dilution of the active ensembles by atoms of an inert group IB metal was found to improve e.g. selectivity toward isomerization and aromatization (*5, 6*). The surface of bimetal particles of this category is often enriched in the group IB metal (*7*). Therefore, even small additions of a catalytically inert metal to an active metal drastically decrease the propensity of the latter to catalyze hydrogenolytic reactions (*8*). The present work deals with a zeolite-supported bimetal system: (Pd + Cu)/NaY. Attention will be focused on the following points:

(i) Enhancement of the reducibility of Cu by the presence of Pd in the same zeolite;

(ii) Formation of bimetallic PdCu particles in supercages;

(iii) Selective oxidation of Cu atoms in PdCu particles by zeolite protons;

(iv) Hydride formation of Pd or PdCu as a function of composition and particle size.

Interest in the first two points is motivated by previous results obtained in this laboratory with (Pt + Cu)/NaY (*9*) and (Pd + Co)/NaY (*10, 11*). The reader is referred to these papers. For the system (Pd + Ni)/NaY reducibility enhancement and mechanisms of alloy particle formation have been identified recently (*12*). In each of these systems relevant information was obtained by the dynamic techniques TPR (temperature-programmed reduction) and TPD (temperature-programmed desorption, mostly of hydrogen) in combination with EXAFS and spectroscopic techniques. The same methods are, therefore, applied in the present work.

Points (iii) and (iv) may require some explanation. Reduction of ion-exchanged metal ions in zeolites results in the formation of metal particles and protons. These strongly acidic protons not only provide bifunctionality to the reduced metal/zeolite catalysts, but they also are able to intereact with the metal particles. Recently it has been shown, for example, that protons react with PtCu bimetal clusters by selectively oxidizing the Cu atoms. The Cu^{2+} ions formed in this "leaching" process tend

0021-9517/91 $3.00

to migrate towards smaller zeolite cages, as follows from recent EXAFS data of Tzou *et al.* (*14*). Reoxidation of Cu during purging in an inert gas atmosphere is favored by a high concentration of protons. Dihydrogen is formed by this oxidative leaching:

$$Cu_{\text{in CuPt particle}} + H^+ \rightarrow Cu^+ + \tfrac{1}{2}H_2 \quad (1)$$

or

$$Cu_{\text{in CuPt particle}} + 2H^+ = Cu^{2+} + H_2. \quad (2)$$

For the system (Pt + Cu)/NaY this reoxidation can be detected by the release of hydrogen in the TPD mode of catalyst characterization, and by EXAFS. For the system (Pd + Cu)/NaY an additional experimental tool is available: Pd particles form a Pd hydride, which is easily detected, e.g., by the typical H_2 release peak at low temperature, but PdCu alloy particles of high Cu content do not form hydrides. The absence of this hydride peak in the TPD profile therefore proves that alloy formation has been quantitative; presence of the hydride peak reveals that Cu has been leached out. Therefore monitoring of the characteristic hydride peak is an essential part of this work.

However, there is some controversy in the literature about the ability of very small Pd particles to form bulk hydrides. Therefore a brief discussion of this particle size effect has been included in this paper.

II. EXPERIMENTAL

A. *Sample Preparation*

Three bimetal samples of $PdCu_x/NaY$ ($x = 0.52, 1.02, 1.89$) have been prepared by ion exchange and analyzed by atomic absorption. One sample was analyzed by Galbraith Laboratory, Inc.; their report is consistent with our in-house analysis. The loadings of the three samples and the average stoichiometry of the alloys are compiled in Table 1, together with the short labels used further in this paper.

Union Carbide zeolite NaY (LZY-52) was used as the support. The Pd and Cu precursors are $Pd(NH_3)_4(NO_3)_2$ and $Cu(NH_3)_4SO_4$ (Alfa Products), respectively. Ion exchange was carried out by dropwise addition of 0.01 *M* of ionic precursor solutions to a constantly stirred NaY slurry [200 ml doubly deionized water (DDW) per gram of NaY]. Each ion exchange was maintained for another 24 h after complete addition of the precursor solution. After ion exchange, an aqueous solution of ammonia with pH = 10.5 was used to repeatedly wash the samples during filtration. The samples were then dried at ambient temperature and stored in a desiccator above a saturated NH_4Cl solution.

TABLE 1

Composition of Bimetal Samples

Weight load (%)		Alloy stoichiometry	Label
Pd	Cu		
3.44	1.09	$PdCu_{0.52}$	PdCu–0.5
3.37	1.98	$PdCu_{1.02}$	PdCu–1
3.57	4.08	$PdCu_{1.89}$	PdCu–2

B. *Characterization by Dynamic Methods*

A program was devised of several sequential TPR and TPD runs, where TPR means programmed heating in a flow of 5% H_2 in Ar and TPD means programmed heating, either in the same gas or in a pure Ar flow. This program provided information on first reduction of the metals, reoxidation of part of the Cu by protons, desorption of chemisorbed hydrogen, and decomposition of metal hydrides. Prior to the first reduction, all samples were calcined to a specified temperature (T_c) under high oxygen flow (2000 ml/min per gram of sample) and a low heating rate (0.5°C/min). The heating rate during TPR and TPD was 8°C/min. For each sample, first TPR was performed by starting from −78°C after Ar purge at T_c following calcination. After the first TPR, the sample was cooled under H_2/Ar (5% H_2) to −78°C. This was followed by the first

TPD in H_2/Ar (5% H_2) stream. This step was intended to detect any hydride formed, while maintaining a constant H_2 partial pressure. After the first TPD, the samples were cooled in H_2/Ar and purged with pure Ar at room temperature for 20 min. A second TPD was conducted in pure Ar starting from −78°C. The purpose of this TPD run was to measure the desorption of chemisorbed hydrogen, as well as hydrogen evolved by the reoxidation of Cu. After the second TPD, the samples were cooled to room temperature under Ar. H_2/Ar was introduced at room temperature and the sample was cooled in this atmosphere to −78°C. A following second TPR run served two purposes: detection of a hydride phase, if present, and re-reduction of Cu that had been re-oxidized during the second TPD. Hydrogen evolution from hydride decomposition was registered as a negative peak in the TPR graph of hydrogen consumption vs time and temperature. Finally, a third TPD run under H_2/Ar was performed to detect any hydride phase that might have formed during cooling in H_2/Ar after the second TPR. In Table 2, the TPR and TPD conditions are summarized.

In some cases, the protons generated during hydrogen reduction of the metals were neutralized with $NaOH_{aq}$ in a nitrogen atmosphere. For this purpose, the samples were sealed in a reactor with teflon stopcocks after calcination to 500°C and reduction to 500°C. They were then exposed to a deoxygenated DDW reservoir for hydration and transferred to a glove bag, where neutralization was performed. About 500 mg of the sample was put in a 700 ml aqueous NaOH solution of initial pH = 10.5; the slurry was stirred for 12 h. Another 500 ml NaOH pH = 10.5 solution was used to wash the sample during filtration inside the glovebag. The pH value of the filtrate was about 7. This corresponds to a neutralization of approximately 75% of the protons in the sample. We shall refer to this as first neutralization. A second neutralization was performed in a similar way. The final pH value of the second filtrate was about 8. After neutralization, the samples were dried and loaded into the reactor inside the glovebag. Subsequent TPR showed that neither Pd nor Cu had been oxidized during the neutralization procedure.

TABLE 2

TPR and TPD Conditions

Sequence	Gas(es)	Temperature range (°C) (min)[a]	Time
1st TPR	H_2/Ar	−70 to 500	60
1st TPD	H_2/Ar	−70 to 100	0
2nd TPD	Ar	−70 to 500	40
2nd TPR	H_2/Ar	−70 to 500	20
3rd TPD	H_2/Ar	−70 to 100	0

[a] Time that sample was held at final temperature.

C. EXAFS Data Collection

X-ray absorption measurements were performed for Pd K-edge (24350eV) at the X-11A of NSLS at Brookhaven National Lab. Each sample of about 500 mg was maintained at liquid nitrogen temperature during each measurement, using the EXAFS transmission cell described previously (*14, 15*). The synchrotron energy and current were typically 2.5 GeV and 200 mA, respectively. A Si(111) monochromator was used.

Two samples of PdCu–1 were prepared. Both were calcined to 500°C and reduced to 450°C. One sample was cooled in H_2 stream to room temperature after reduction. This sample will be referred to as PdCu/500/450/H_2. Another sample was purged with He at 450°C for 30 min and was cooled under He flow at the end of the reduction. This sample will be referred to as PdCu/500/450/He. The sample transfer procedure has been described elsewhere (*14, 15*).

III. RESULTS

A. Enhanced Reducibility of Copper

The TPR profile for monometallic Cu/NaY is shown in Fig. 1. The hydrogen con-

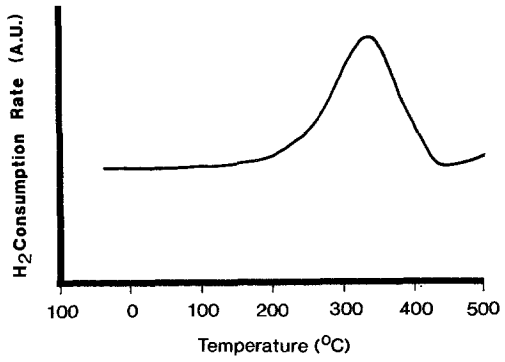

FIG. 1. TPR profile of CuNaY.

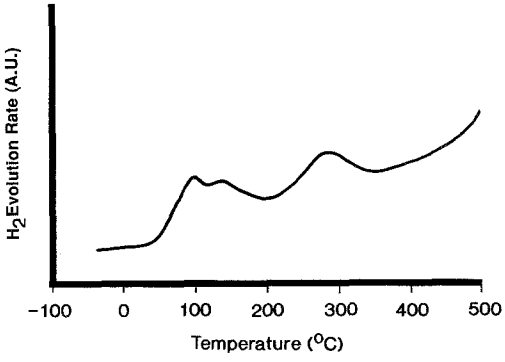

FIG. 3. Second TPD profile of PdCu–1.

sumption corresponds to about 60% of that needed for complete reduction of Cu^{2+} ions to metallic Cu. No H_2 evolution was detected in subsequent TPD runs 1 and 2. The absence of reoxidation during TPD was confirmed in a second TPR run: no H_2 consumption was detected.

Figure 2 shows the TPR profiles of PdCu–1 after two calcination programs: trade A (solid line) after T_c = 250°C and trace B (dashed) after T_c = 500°C. Integration of these profiles indicates complete reduction of both Pd^{2+} and Cu^{2+} to their metallic states at 500°C. There are two major differences: (i) the main reduction peak for the sample calcined at T_c = 250°C is at 190°C, but the sample calcined at 500°C has its main reduction peak at 170°C; (ii) reduction of Cu ions is completed below 400°C for the sample calcined at 250°C, but the T_c = 500°C sample has a peak at 400°, corresponding to the reduction of the last 30% of the Cu^{2+}. No hydride peak is detected in the first TPD of either sample. Their second TPD profiles are also similar; one is shown in Fig. 3. Three major peaks are observed. Since they overlap, we have refrained from attempting an integration of individual peaks.

The impression that some re-oxidation by protons contributes to the hydrogen evolution in Fig. 3 was confirmed by subsequent TPR experiments shown in Fig. 4. The H_2 consumption and the peak position both depend on the severity of the preceding 2nd TPD program; if it was terminated at 350°C, TPR profile A is obtained, but if

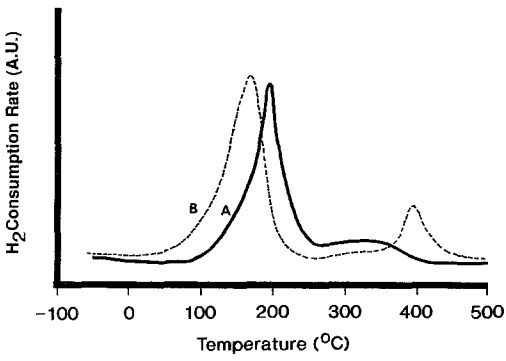

FIG. 2. TPR profiles of PdCu–1 after calcination at 250°C (A) and after calcination at 500°C (B).

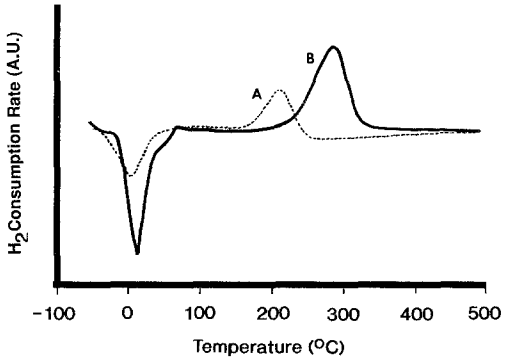

FIG. 4. Second TPR profiles of PdCu–1 after interrupting second TPD at 350°C (A) and after second TPD without interruption (B).

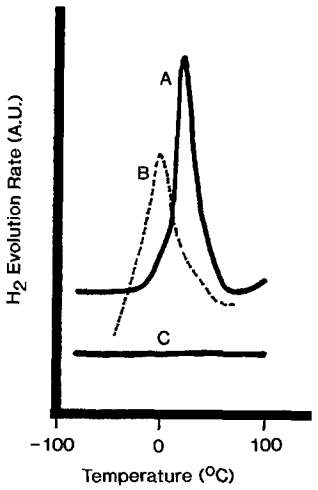

FIG. 5. First TPD profiles of PdNaY (A), PdCu–0.5 (B), PdCu–1 and PdCu–2 (C).

carried up to 500°C, profile B in Fig. 4 is observed.

For samples PdCu–2 and PdCu–0.5, the TPR profiles after T_c = 250 and 500°C are similar to those of PdCu–1, taken at identical conditions. A major difference is that in comparison to PdCu–1 the H_2 consumption at 400°C after T_c = 500°C is higher for PdCu–2, but lower for PdCu–0.5. After T_c = 250°C the reduction of Cu^{2+} ions is more enhanced for PdCu–0.5 than for PdCu–1.

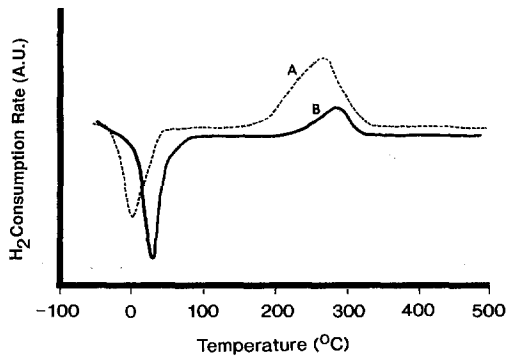

FIG. 6. Second TPR profiles of PdCu–2 (A) and PdCu–0.5 (B).

B. Cu Leaching and Hydride Formation

Hydrides are detected in two ways: (i) As positive H_2 evolution peaks at low temperature in TPD profiles; (ii) as negative H_2 consumption peaks in "2nd TPR" plots. Note that before these plots were taken, Pd was reduced and the sample had been exposed to H_2/Ar at −78°C.

In Fig. 5, first TPD plots (i.e., after reduction and cooling in H_2) are given for pure Pd (trace A), PdCu–0.5 (trace B), and PdCu–1 and PdCu–2 (trace C). It is clear that the latter two samples do *not* form hydrides. This shows that alloy formation is complete; any un-alloyed Pd should reveal itself by a hydride peak.

The "2nd TPR" profiles of PdCu–2 and PdCu–0.5 are shown in Fig. 6 as trace A (dashed line) and trace B (solid line), respectively. The negative peak indicating hydride decomposition appears at 3°C for PdCu–2, and that at 32°C is for PdCu–0.5. Apparently, Cu had been leached out of the bimetal particles during the 2nd TPD treatment; the Cu^{2+} ions are re-reduced in the 2nd TPR run. Both the leaching and the re-reduction are apparently quantitative: the hydrogen consumption for the re-reduction of this Cu^{2+} is four times higher for the former than for the latter sample, as expected.

The hydride/Pd ratios of PdCu–2, PdCu–1, and PdCu–0.5 obtained at various stages are listed in Table 3. The numbers obtained for T_c = 250°C have been reproduced for T_c = 500°C within 5% error for all samples,

TABLE 3

Hydride/Pd Ratios[a]

PdCu-	1st TPD	2nd TPR	3rd TPD
2	0	0.20 (3)	0
1	0	0.24 (17)	0
0.5	0.16 (7)	0.32(32)	—
Pd	0.20 (15)	0.38 (32)	—

[a] Numbers in ( ) are the hydride decomposition temperatures in °C.

i.e., the numbers in Table 1 represent both calcination temperatures.

The implicit assumption that zeolite protons are responsible for oxidative leaching of Cu is verified by repeating the above experiments with samples that had been neutralized with aquous NaOH. Indeed, neutralized PdCu–1 did not show any H_2 consumption in subsequent TPR, nor did the first TPD show any hydride decomposition. The profiles of the second TPD are shown in Fig. 7 for a sample after first and second neutralization as traces A and B, respectively. Clearly, the second major peak of Fig. 3 is absent in Fig. 7, indicating that this peak represents H_2 evolution due to reactions (1) or (2). When the neutralized samples were subjected to a second TPR program, the profiles displayed in Fig. 8 are registered for first (trace A) and second (B) neutralization. Comparison of these with Fig. 4 reveals two major differences: First, the neutralized samples do not show the low temperature hydride peak. Second, H_2 consumption for reduction of leached Cu^{2+} ions is negligible; the measured numbers (3% and 1% instead of 17%) are within our experimental error of 10%.

The k^2 weighted EXAFS functions of PdCu/500/450/H_2 (cooled in H_2 after reduction) and PdCu/500/450/He (purged with He at 450°C for 30 min and cooled in He) are shown in Fig. 9A and 9B, respectively. Their Fourier transforms within the k range of 3–16 $Å^{-1}$ are displayed in Fig. 10A and 10B, respectively. For sample PdCu/500/450/H_2, a smooth shoulder to the low R(Å) side of the main peak (Pd–Pd bond) in Fig. 10A is due to Pd–Cu bond. However, Fig. 10B shows mainly bonding between first nearest Pd–Pd neighbors. Theoretical fittings to the experimental data in the inverse Fourier transforms between 1.6 and 2.85 Å for PdCu/500/450/H_2 and PdCu/500/450/He are shown in Fig. 11A and Fig. 11B, respectively. The fitted parameters are listed in Table 4.

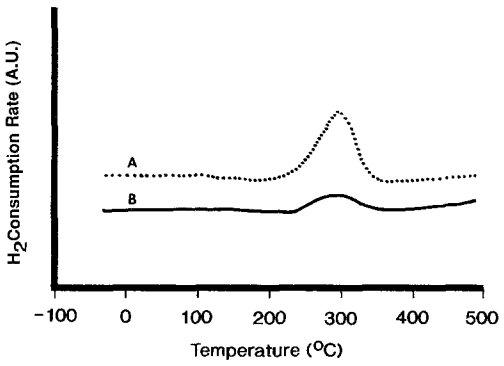

FIG. 8. Second TPR profiles of PdCu–1 after first neutralization (A) and after second neutralization (B).

IV. DISCUSSION

A. Enhanced Reducibility of Copper

Copper ions in monometallic Cu/NaY are only partially reduced below 450°C.

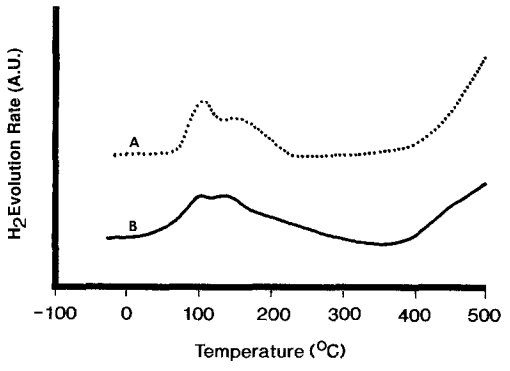

FIG. 7. Second TPD profiles of PdCu–1 after first neutralization (A) and after second neutralization (B).

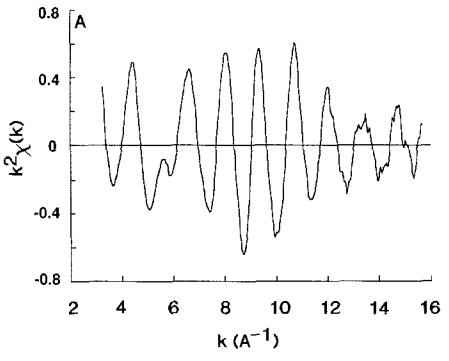

FIG. 9A. k^2-weighted EXAFS $\chi(k)$ function for PdCu/500/450/H_2.

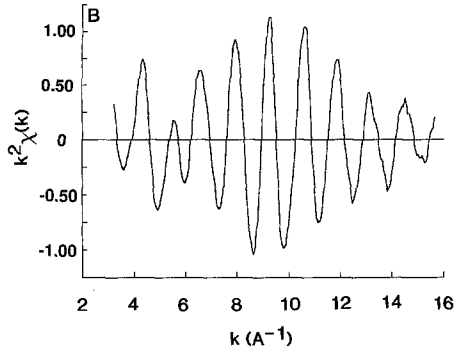

FIG. 9B. k^2-weighted EXAFS $\chi(k)$ function for PdCu/500/450/He.

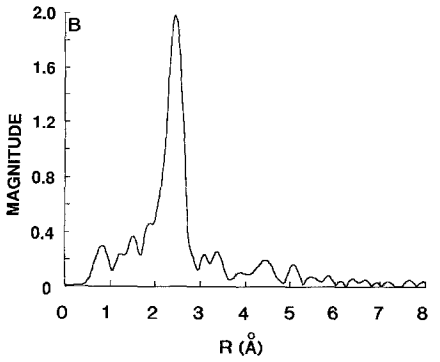

FIG. 10B. Fourier transform of $k^2\chi(k)$ function for PdCu/500/450/He.

Figure 1 suggests that reduction of Cu^{2+} ions in the absence of Pd does not proceed beyond the stage of Cu^+. This is in conformity with results of other authors (*9, 16*). Since the pH of the ion exchange solution was adjusted with ammonia, partial exchange of Na^+ ions by NH_4^+ was expected. After calcination, the sample resembles Cu/NaHY. In acidic zeolites, reduction of Cu^+ is known to require high temperature.

The reduction of PdCu/NaY strongly depends on the relative locations of the ionic precursors. For the sample calcined to 250°C, it was shown previously that *cis*-$Pd(NH_3)_2^{2+}$ ions are the prevailing species in supercages (*17*). Temperature-programmed oxidation of $Cu(NH_3)_4^{2+}$/NaY showed a broad oxygen consumption peak and a nitrogen evolution peak, mirror-imaged at 350°C (data not shown). An interaction of Pd and Cu ions in supercages is, therefore, expected after calcination up to T_c = 250°C. This type of interaction has been reported for $Pd(NH_3)_2^{2+}$ and $Co(NH_3)^{2+}$ ions in the supercages of zeolite Y (*11*).

The TPR profile for PdCu/NaY after calcination to T_c = 250°C suggests reduction of all Pd ions together with some Cu ions; these are probably located in the near vicinity of Pd, so that they can easily migrate toward reduced PdCu particles. The enhancement of the reduction of Cu by Pd is evidenced by the complete reduction of Cu^{2+} ions to Cu^0 below 400°C. X-ray diffraction studies have shown that, after high temperature calcination, Cu^{2+} ions are distributed over sodalite cages and hexagonal

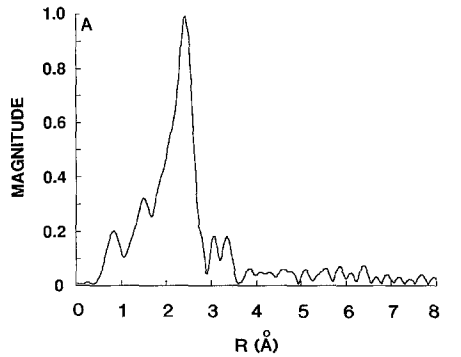

FIG. 10A. Fourier transform of $k^2\chi(k)$ function for PdCu/500/450/H_2.

TABLE 4

EXAFS Parameters

	PdCu/500/450/H_2			PdCu/500/450/He		
	N	R(Å)	$\sigma \times 10^2$	N	R(Å)	$\sigma \times 10^2$
Pd–Cu	0.94	2.58	0.8	0.5	2.60	0.4
Pd–Pd	1.58	2.72	1.0	3.47	2.74	0.9
Pd–O	2.3	2.22	2.7	1.74	2.25	2.6

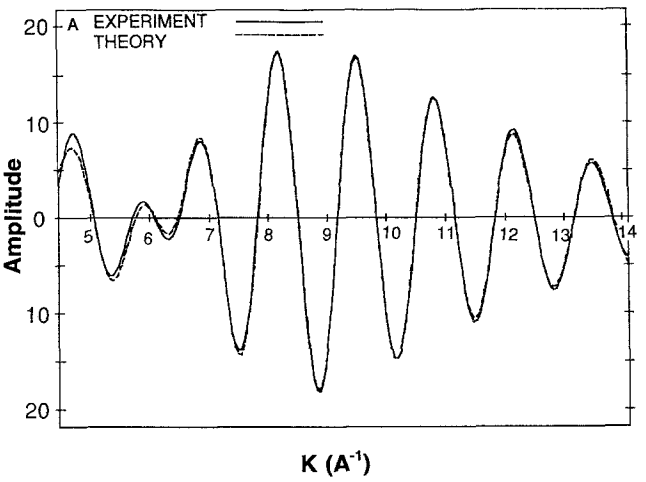

FIG. 11A. Curve fitting for the EXAFS function of PdCu/500/450/H_2.

prisms (*18*). For the PdCu/NaY sample that was calcined to 500°C, most Cu^{2+} ions share sodalite cages with Pd^{2+} ions. Simultaneous reduction of the paired ions takes place at 170°C. A minor fraction of Cu ions (<30%) is reduced at 400°C. These Cu ions are presumably located in hexagonal prisms. It follows that a similar proximity requirement is valid as previously demonstrated for the enhanced reduction of Co^{2+} ions by Pd in zeolite Y (*11*).

B. Cu Leaching and Hydride Formation

Palladium metal is known to exothermically form hydrides (*19, 20*). Two hydride phases are normally distinguished:

α Pd hydride; heat of solution: 6.0–8.8 kcal/mol (H_2),

β Pd hydride; heat of solution: 9.7 kcal/mol (H_2).

For bulk Pd metal, both phases co-exist in equilibrium at normal conditions. The criti-

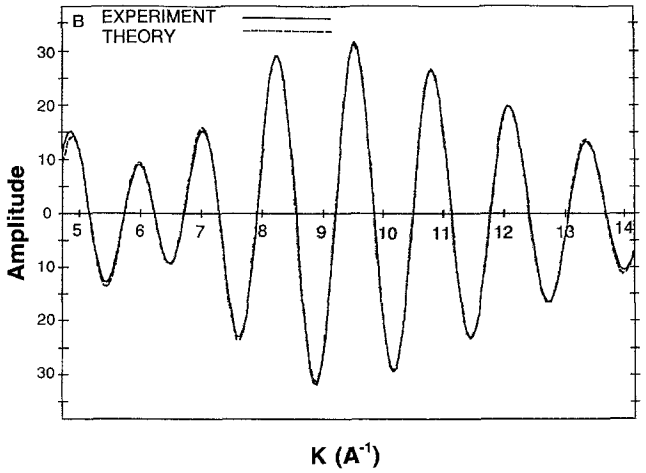

FIG. 11B. Curve fitting for the EXAFS function of PdCu/500/450/He.

cal temperature at which the two-phase region disappears is 295°C for the Pd–H_2 system at p_{H_2} = 14 atm (*19, 21*). It is also known that the H/Pd ratio is a function of H_2 partial pressure. In the present study, a constant partial pressure of p_{H_2} = 38 torr was maintained during TPR.

No hydrogen is absorbed by copper at low temperature, (*22, 23*) because hydrogen absorption in copper is endothermic (*24*). For bulk Pd–Cu alloys it has been well established that H_{abs}/Me decreases rapidly with increasing Cu content (*25*). At a H_2 partial pressure of 38 torr, for example, the H_{abs}/Me ratio becomes zero for a Cu concentration in a bulk Pd–Cu alloy above 20% (*25*).

For most supports, bimetal catalysts consisting of Cu and any of the transition metals Ni, Pt, Ir, Ru, or Os, surface segregation of Cu has been observed, i.e., the surface of the bimetal particles is generally enriched with Cu (*7, 26, 27*). A similar structure of bimetallic PtCu particles in zeolite Y has been determined very recently (*13*). It is possible that a Cu-rich surface inhibits hydride formation even for those alloys where it is thermodynamically possible.

In the presentation of EXAFS results, the average number of neighbor atoms forming bonds with a central X-ray absorbing atom is generally referred to as coordination number N. In the present study, Pd atoms are absorbers. After cooling in H_2, the completely reduced samples, e.g., PdCu/500/450/H_2, show a ratio of the coordination numbers N_{Pd-Cu}/N_{Pd-Pd} = 0.94/1.58. On the other hand, after heating in He, sample PdCu/500/450/He has a N_{Pd-Cu}/N_{Pd-Pd} ratio of 0.50/3.47. Evidently, the Cu concentration in the bimetallic particles of PdCu/500/450/He is significantly decreased with respect to that of PdCu/500/450/H_2. This EXAFS result is in line with recent EXAFS data by Tzou *et al.* that showed that Cu atoms are leached from PtCu bimetal particles in zeolite Y under He (*14*).

The typical EXAFS error in the bond distances is 0.02 Å and the error in the coordination numbers is ±20%. It is known that the coordination number is very sensitive to changes of particle size when particles are small. For large particles, the coordination number becomes less sensitive to variations in particle size. In the present zeolite system, the encaged (bi)metal particles are extremely small, as indicated by the small coordination numbers. The evaluation of metal particle sizes is therefore fairly reliable.

The present results show that the leaching of Cu can be detected by hydride formation of the Pd particle. The absence of the hydride phase in the first TPD and the detection of the hydride phase in the second TPR (Fig. 4) indicate that a hydride phase is formed only after Cu atoms are leached from the PdCu bimetal particles. The mechanism of the Cu leaching process under He is evidenced by the 2nd TPD profile of Fig. 3 and the 2nd TPR profiles of Fig. 4. The first peak in Fig. 3 is due to the desorption of chemisorbed hydrogen. The second peak at 280°C, though still in the region where chemisorbed hydrogen is desorbed, is actually due to oxidative Cu leaching by protons. This follows from a crucial experiment where the temperature was stopped at 350°C in the 2nd TPD. Subsequent TPR (Fig. 4; trace A) shows reduction of Cu ions at 210°C and a weak hydride release at 4°C. When the 2nd TPD was carried out to 500°C followed by holding for 40 min, the subsequent second TPR profile (Fig. 4B) shows an evolution of hydrogen at 17°C due to hydride decomposition and the reduction of leached Cu^{2+} ions at 290°C. The quantitative results of the hydride phase give a H_{abs}/Pd ratio of 0.24. The lower Cu reduction temperature in traces A and B of Fig. 4 is ascribed to different locations of Cu ions after reoxidation at different temperatures in the 2nd TPD. Reoxidation of Cu possibly occurs in two steps:

$$Cu^{\circ}Pd_x + H^+ \rightarrow Cu^{+}Pd_x + \tfrac{1}{2}H_2 \quad (3)$$

$$nCu^{+}Pd_x + nH^+ \rightarrow nCu^{2+} + Pd_{nx} + \tfrac{1}{2}nH_2 \quad (4)$$

The first reoxidation peak (maximized at 280°C) of Fig. 3 is likely due to step (3). The resulting Cu^+ ions are isoelectric with Ni. The enhanced reduction of Cu^+ ions (reverse of Eq. (3)) at 210°C (trace A of Fig. 4) suggests that they are still in close contact with Pd.

After reoxidation at high temperature (500°C), Cu^{2+} ions will migrate into sodalite cages and hexagonal prisms in step (4). Their reduction can only be enhanced if they migrate back to Pd particles in supercages. Indeed, the subsequent reduction of leached Cu^{2+} then occurs at a significantly higher temperature (290°C, trace B of Fig. 4). As a result of the formation of bimetallic particles after this second TPR, hydride formation is again absent.

The suppression of hydride formation by Cu on Pd particles in zeolite cages has been further supported by the samples of PdCu–2 and PdCu–0.5. For the sample PdCu–0.5, a hydride decomposition peak was observed even in the first TPD. The low H/Pd ratio (0.16) and the low decomposition temperature (7°C) suggest that the hydride phase is less stable than that after second TPD, where a H/Pd ratio of 0.32 and a decomposition temperature of 32°C are detected after Cu leaching. On the other hand, reduced PdCu–2 is unable to form hydride. Only after Cu atoms are oxidatively leached from PdCu bimetal particles can a hydride be formed. A comparison of the 2nd TPR profiles of samples PdCu–0.5 and PdCu–2 in Fig. 6 is of relevance: since PdCu–0.5 has four times less Cu than PdCu–2, the peak corresponding to the reduction of reoxidized Cu is much smaller for the former than for the latter.

All experimental criteria showing oxidative leaching of Cu and formation of Pd hydride after leaching are virtually absent for samples in which the zeolite protons have been neutralized. This leaves little doubt that these protons are the oxidizing agents. The high temperature peak in Fig. 7 is likely due to reoxidation of Cu by protons in sodalite cages or hexagonal prisms. The migration of protons to supercages is an activated process. At room temperature where neutralization is carried out, protons in these hidden sites might survive.

The EXAFS data reveal that the average particle sizes of samples PdCu/500/450/H_2 and PdCu/500/450/He are smaller in comparison to the reported results on Pd/NaY (*14*). Bimetallic particles in PdCu/500/450/He are larger than in PdCu/500/450/H_2. This might be a consequence of metal anchoring by the additional protons that are formed during the reduction of Cu. Our recent studies with EXAFS and FTIR showed that protons in zeolite anchor primary small Pd particles to the cage walls (*14, 28*). After reduction, the average composition of bimetal particles corresponds approximately to $CuPd_2$ and $CuPd_3$. These particles are unable to form hydrides. For PdCu/500/450/He, the proton concentration is reduced in the process of Cu reoxidation. The resulting Cu^{2+} ions migrate into sodalite cages and hexagonal prisms. After step (4), the coordination numbers of $N_{Pd-Cu} = 0.5$ and $N_{Pd-Pd} = 3.5$ can be approximately translated to an average particle composition of Pd_6Cu_1. It is remarkable that particles of Pd_6Cu_1 are capable of forming a hydride. The absence of the hydride phase demonstrated by the third TPD after the reduction of the reoxidized Cu ions shows again the suppression of hydride formation by Cu in PdCu bimetal particles.

It has been reported that the solubility of H_2 in supported Pd at a given pressure and temperature decreases with decreasing particle size and that formation of the β hydride is structure-sensitive for small Pd particles (*29*). With large Pd particles on SiO_2 support, β-hydride was observed with X-ray diffraction (XRD) (*30*). Benedetti *et al.* report detection of β-hydride with Pd particles of about 25 Å supported on charcoal (*31*). However, the lack of evidence for hydride formation of small Pd particles with dispersions above 50% is mainly due to the limitation of XRD for small particles (*30*). Pd hydride was detected in zeolite Y supported Pd particles as small as 10 Å by the expansion of the Pd–Pd distance with

EXAFS and small angle scattering techniques (*32*). The H_{abs}/Pd ratio of 0.4 for pure Pd in zeolite Y reported by Moraweck *et al.* (*32*) is very close to our value of 0.38 listed in Table 2. However, our TPD profile as shown in Fig. 5 indicates that α-hydride prevails and that the amount of β-hydride is negligible. The TPD peak at 80°C, which is characteristic for β-hydride, is not observed in this case. In the present system, with particles of an average size of six Pd atoms, the limit of hydride formation is demonstrated. While the β-hydride phase has been found for bulk Pd metal, the hydride detected in the present study is of type α, although this distinction becomes almost semantic for such small clusters.

V. ACKNOWLEDGMENTS

Financial support by the Department of Energy under contract DE-FG02-87ER13654 is gratefully acknowledged. We also thank Professor E. Stern for kindly donating his EXAFS package.

VI. REFERENCES

1. Ponec, V., and Sachtler, W. M. H., *J. Catal.* **24,** 250 (1972).
2. Sachtler, W. M. H., *Vide* **163–165,** 19 (1973).
3. Beelen, J. M., Ponec, V., and Sachtler, W. M. H., *J. Catal.* **28,** 376 (1973).
4. Sachtler, W. M. H., and Van Santen, R. A., *Adv. Catal.* **26,** 69 (1977).
5. Sinfelt, J. H., *J. Catal.* **29,** 308 (1973).
6. Sinfelt, J. H., Lam, Y. L., Cusumano, J. A., and Barnett, A. E., *J. Catal.* **42,** 227 (1976).
7. van der Plank, P., and Sachtler, W. M. H., *J. Catal.* **7,** 300 (1967).
8. Sinfelt, J. H., *Catal. Rev.* **9,** 147 (1974).
9. Moretti, G., and Sachtler, W. M. H., *J. Catal.* **115,** 205 (1989).
10. Zhang, Z., Sachtler, W. M. H., and Suib, S. L., *Catal. Lett.* **2,** 395 (1989).
11. Zhang, Z., and Sachtler, W. M. H., *J. Chem. Soc. Faraday Trans.* **86,** 2313 (1990).
12. Feeley, J. S., and Sachtler, W. M. H., submitted.
13. Tzou, M. S., Kusunoki, Asakura, K., Kuroda, H., Moretti, G., and Sachtler, W. M. H., *J. Phys. Chem.,* accepted.
14. Zhang, Z., Chen, H., Sheu, L. L., and Sachtler, W. M. H., *J. Catal.* **127,** 213 (1991).
15. Zhang, Z., Chen, H., and Sachtler, W.M. H., *J. Chem. Soc. Faraday Trans.,* **87,** 1413 (1991).
16. Petunchi, J. O., and Hall, W. K., *J. Catal.* **80,** 403 (1983).
17. Zhang, Z., Sachtler, W. M. H., and Chen, H., *Zeolites* **10,** 784 (1990).
18. Gallezot, P., Ben Tarrit, Y., Imelik, B., *J. Catal.* **26,** 161 (1972).
19. Mueller, W. M., Blackledge, J. P., and Libowitz, G. G., "Metal Hydrides." Academic Press, New York/London, 1968.
20. Lewis, F. A., "The Palladium Hydrogen System." Academic Press, New York/London, 1967.
21. Wicke, E., and Brodowsky, H., *in* "Topics in Applied Physics," (G. Alefeld and J. Völkl, Eds.), Vol. 29, p. 73. Springer-Verlag, Berlin/New York, 1978.
22. Benton, A. F., *Trans. Faraday Soc.* **28,** 202 (1932).
23. Kington, G. L., and Holmes, J. L., *Trans. Faraday Soc.* **49,** 417 (1953).
24. Mueller, W. M., Balckledge, J. P., and Libowitz, G. G., "Metal Hydrides," p. 82. Academic Press, New York/London, 1968.
25. Karpova, R. A., and Tverdovskii, I. P., *Zh. Fiz. Khim.* **333,** 1393 (1959).
26. Via, G. H., Drake, K. F., Jr., Meitzner, G., Lytle, F. W., and Sinfelt, J. H., *Catal. Lett.* **5,** 25 (1990).
27. Sinfelt, J. H., *Acc. Chem. Res.* **10,** 15 (1977).
28. Zhang, Z., Wong, T., and Sachtler, W. M. H., *J. Catal.,* **128,** 13 (1991).
29. Boudart, M., and Hwang, H. S., *J. Catal.* **39,** 44 (1975).
30. Pitchai, R., Wong, S. S., Takahashi, N., Butt, J. B., Burwell, R. L., Jr., and Cohen, J. B., *J. Catal.* **94,** 490 (1985).
31. Benedetti, A., Cocco, G., Enzo, S., Pinna, F., and Schiffini, L., *J. Chim. Phys., Phys.-Chim. Biol.* **78,** 875 (1981).
32. Moraweck, B., Clugnet, G., and Renouprez, A., *J. Chim. Phys.* **83,** 265 (1986).